Polymer 55 (2014) 1481–1490

Contents lists available at ScienceDirect

Polymer

journal homepage: www.elsevier.com/locate/polymer

Honeycomb-like polymeric films from dendritic polymers presenting reactive pendent moieties

Yu-An Su [a], Wei-Fan Chen [b], Tzong-Yuan Juang [c,*], Wei-Ho Ting [b], Ting-Yu Liu [d], Chi-Fa Hsieh [e], Shenghong A. Dai [b], Ru-Jong Jeng [a,**]

[a] *Institute of Polymer Science and Engineering, National Taiwan University, Taipei 106, Taiwan*
[b] *Department of Chemical Engineering, National Chung Hsing University, Taichung 402, Taiwan*
[c] *Department of Applied Chemistry, National Chiayi University, 300 Syuefu Road, Chiayi 60004, Taiwan*
[d] *Department of Materials Engineering, Ming Chi University of Technology, New Taipei City 243, Taiwan*
[e] *Chung-Shan Institute of Technology, Lungtan, Taoyuan 325, Taiwan*

ARTICLE INFO

Article history:
Received 28 September 2013
Received in revised form
13 January 2014
Accepted 25 January 2014
Available online 11 February 2014

Keywords:
Dendrons
Honeycomb
Crosslinking

ABSTRACT

In this paper we describe the fabrication of honeycomb-shaped polyurethane films from dendritic side-chain polymers presenting reactive pendent units. Two novel functional polyurethanes, poly(urethane-*co*-acylurea) (**PU-PACY**) and polyurethane-co-azetidine-2,4-dione containing polyurethane (**PU-PAZ**), were synthesized. The waxy dendrons featured focal urea/malonamide linkages favorable for hydrogen bonding and peripheral alkyl chains. These intermolecular forces caused two functional PUs to undergo phase separation and self-assembly. This resulted in honeycomb-like films with well-controlled surface roughness characterized in terms of the ratio of rim width (W) to the pore size (D), i.e. W/D. The **PU-PAZ** film had a higher contact angle (CA) and a lower value of W/D than did the **PU-PACY** analogue, due to the presence of relatively more hydrophobic azetidine-2, 4-dione functionalities in the former film. Subsequent chemical modification of the **PU-PAZ** films through reaction with a hydrophobic poly(oxyalkylene) amine enhanced the CA from 113 to 134°. Further physical modification through a peeling-off process rendered the film surface with a three-dimensional (3D) rod-*co*-valley-structure having feature dimensions on a submicrometer scale. The 3D rod-*co*-valley–like film exhibited superhydrophobicity with a CA of 151°. The films also displayed excellent solvent-resistance after crosslinking with a diamine. Through hydrophobic or hydrophilic chemical modification, we could readily manipulate the surface properties of these honeycomb-like films with controllable surface roughnesses and reactive functionalities.

1. Introduction

Many superhydrophobic materials that mimic the water-repelling surface of the lotus leaf have been reported recently [1–11]. The preparation of these surfaces has relied mainly on two co-operative effects: surface modification to impart low surface energy and the introduction of particular surface morphologies. These morphologies, either two-dimensional (2D) or three-dimensional (3D), have been achieved by implementing such processes as etching, dip-coating, chemical vapor deposition, and molecular self-assembly [12–24]. Molecular self-assembly is particularly interesting because of the possibility of fabricating highly regular structures, such as a honeycomb-like surfaces via a breath-figure process (pioneered by Francois and co-workers) [14,15]. In addition, variations in the chemical composition of the films allow the rim width (W) and pore size (D) to be adjusted, thereby manipulating the surface roughness [25–27].

Using this breath-figure technique, a variety of polymers including functional linear polymers [28], star polymers [29–32], amphiphilic copolymers [23,33–35], ionomer macromolecules [36–38], polyion complexes [27,39,40], hyperbranched polymers [41], and dendritic side-chain block copolymers [42–46], have been employed to obtain honeycomb-like polymeric films. Apart from that, Karthaus et al. reported that there were two methods to obtain

---

* Corresponding author. Tel.: +886 5 271 7967; fax: +886 5 271 7901.
** Corresponding author. Tel.: +886 2 3366 5884; fax: +886 2 3366 5237.
E-mail addresses: tyjuang@mail.ncyu.edu.tw (T.-Y. Juang), rujong@ntu.edu.tw (R.-J. Jeng).

http://dx.doi.org/10.1016/j.polymer.2014.01.032

the solvent-resistance honeycomb films [39], one was chemical crosslinking via condensation of maleic anhydride and 1,8-diaminooctane. The other was a photo-crosslinking system using poly(vinyl cinnamate) [47]. Highly ordered honeycomb films were prepared from photo-crosslinkable polymers. The 3-D honeycomb structure was retained under UV irradiation. More recently, Wang and co-workers reported another photo-crosslinked system [48]. Stable porous morphology was achieved by photo-induced crosslinking during the breath-figure formation. The simple crosslinking operation opens the door to facilely fabricate robust microporous polymer films [49,50].

Our research group has taken an alternative approach to the preparation of hydrophobic honeycomb-like films from dendron-grafted polystyrenes and polyurethanes (PUs) through a combination of self-assembly and a breath-figure process [45,46]. These waxy dendrons feature a focal part rich in hydrogen bonding groups and a periphery rich in nonpolar units that undergo van der Waals interactions. As part of our endeavor to enhance the surface properties of these films (i.e., tailored hydrophobicity/hydrophilicity and solvent-resistance), in this study we developed two novel reactive PU polymers: poly(urethane-*co*-acylurea) (**PU-PACY**) and poly-urethane-co-azetidine-2,4-dione containing polyurethane (**PU-PAZ**) [Scheme 1(a) and (b)]. **PU-PACY** presenting pendent aromatic anhydride moieties was synthesized through carbodiimide (CDI) chemistry [51–53], which is used extensively in peptide synthesis. In esterification processes, the use of CDI chemistry is often hampered by a side reaction that converts carboxylic acids to N-acylureas. On the basis of this reaction, we developed a poly-CDI system and subsequently added trimellitic anhydride (TMA) to obtain poly(*N*-acylurea) as an intermediate for further chemical modification (e.g., to enhanced surface properties). In addition, we took further advantage of the selectively reactive azetidine-2,4-dione moiety in the generation-0.5 dendron (G-0.5) (Scheme 2); this unit reacts only with aliphatic primary amino groups. We readily obtained the azetidine-2.4-dione–containing **PU-PAZ** polymer through chain extension of di-*p*-phenyl diisocyanate (MDI) with dendron-containing diols such as [G-1.5]-C18-Diol and [G-0.5]-Diol (Scheme 3). With their reactive pendent functionalities, these dendritic **PU-PACY** and **PU-PAZ** polymers possess side chains rich in not only hydrogen bonding units but also pendent reactive moieties. Thus, the surface properties of these honeycomb-like PU films could be modified through reactions of these functionalities.

According to the literature [54–58], polymers featuring pendent azetidine-2,4-dione or aromatic anhydride units can react rapidly with aliphatic primary amino functional groups. Therefore, in this study, we employed commercially available difunctional poly(oxyalkylene)amines (hydrophilic Jeffamine®M-1000 and hydrophobic Jeffamine®M-2005) as crosslinkers to impart enhanced surface properties (tunable hydrophobicity up to the level of superhydrophobicity and solvent-resistance) to our honeycomb-like films. In addition, the values of *W*/*D* of the honeycomb-like films could also be controlled through the self-assembly of these various functional polymers. Accordingly, these materials have potential applications in, for example, microanalysis, cell growth, and stent tissue engineering.

2. Experimental

2.1. Materials

Dibutyltin dilaurate (DBTDL or T-12), *N*-(3-aminopropyl)diethanolamine (APDEA), and 1,6-diaminohexane were purchased from TCL. The poly(oxyalkylene)amines Jeffamine®M-1000 and Jeffamine®M-2005 (abbreviated herein as M1000 and M2005, respectively) were purchased from Huntsman. *N*,*N*-dimethylformamide (DMF), tetrahydrofuran (THF), dimethylsulfoxide (DMSO), methylene di-*p*-phenyl diisocyanate (MDI), cyclohexane, methanol, xylene, isobutyryl chloride, stearyl alcohol,

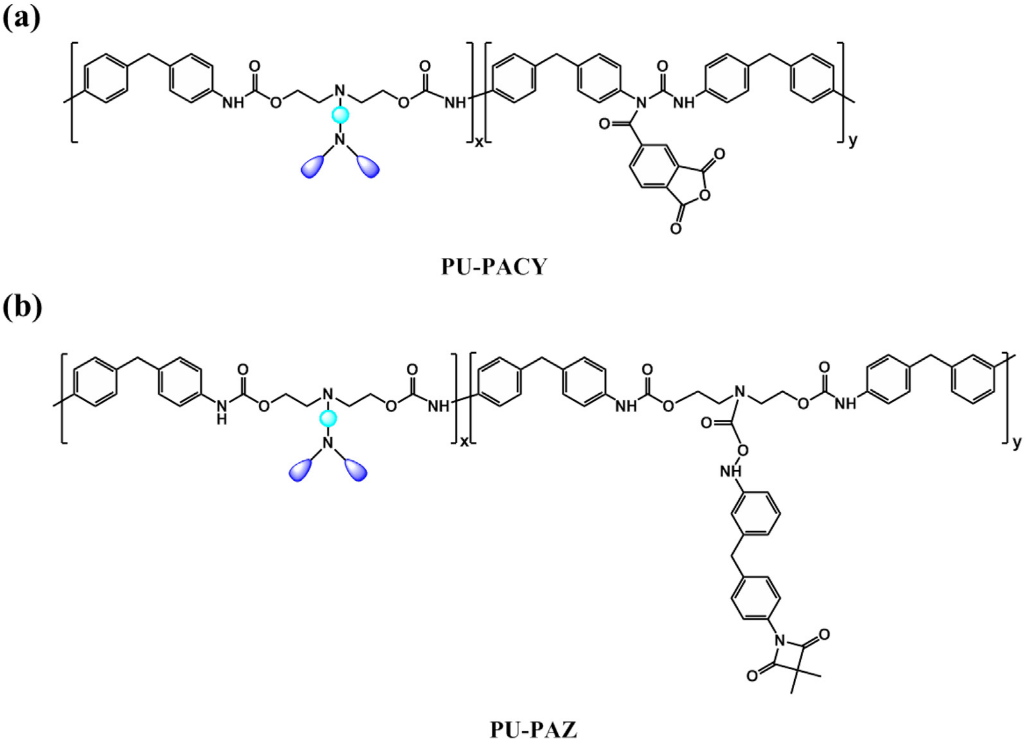

Scheme 1. Chemical structures of (a) **PU-PACY** and (b) **PU-PAZ**.

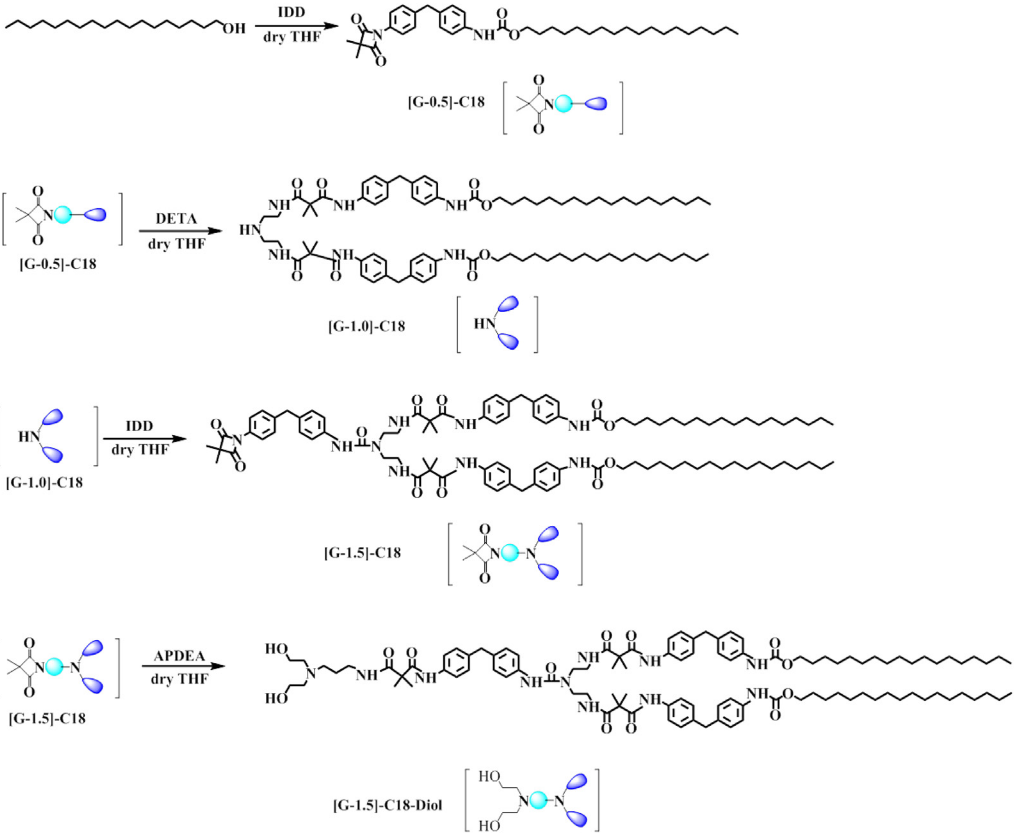

Scheme 2. Syntheses of the [G-0.5]-C18, [G-1.5]-C18, and [G-1.5]-C18-Diol dendrons.

triethylamine (TEA), 1-decanol, and diethylenetriamine (DETA), 1,3-dimethylphosphole 1-oxide (DMPO), and trimellitic anhydride (TMA) were purchased from Aldrich and Acros. Scheme 2 displays the chemical structures of the stearyl ester derivatives of 4-isocyanato-4-(3,3-dimethyl-2,4-dioxo-acetidino)diphenylmethane (IDD) grafted with dendrons of different generations. The building block IDD and the dendrons (from [G-0.5]-C18 to [G-1.5]-C18) were synthesized according to procedures in previous reports [55,59–63].

2.2. [G-1.5]-C18-Diol dendron (Scheme 2)

APDEA (1.00 g, 6.16 mmol) was added dropwise to a solution of [G-1.5]-C18 (2.47 g, 1.40 mmol) in dry THF (25.0 mL). The solution was stirred at 75 °C under a N_2 atmosphere for 48 h. After evaporation of the solvent, the product was purified through recrystallization (MeOH) to give a light-yellow powder (2.23 g, 90.0 %) [Found: C, 68.70; H, 8.22; N, 8.41%. $C_{104}H_{155}N_{11}O_{13}$ requires C, 70.67; H, 8.84; N, 8.72%. FT-IR (ν_{max}/cm^{-1}): 3340 (OH), 1704 [(NH)C=O(O)], 1654 [C=O(NH)]. ^{1}H NMR (400 MHz, CDCl$_3$): δ_H 0.83 (6H, t, CH$_3$), 1.35 [18H, C(CH$_3$)$_2$CONH], 3.78 (6H, PhCH$_2$Ph), 4.0 (4H, NHCOO–CH$_2$), 4.29 (2H, OH), 7.03–7.68 (24H, PhH). FABMS: *m*/*z* 1768 (M$^+$)].

2.2.1. [G-0.5]-Diol dendron (Scheme 3)

Diethanolamine (1.00 g, 9.50 mmol) was added to a solution of IDD (3.80 g, 11.9 mmol) in dry THF (120 mL). The solution was stirred at 0 °C under a N_2 atmosphere for 2 h. After evaporation of the solvent, the product was purified through precipitation from cyclohexane to give a white powder (3.50 g, 86.7%) [Found: C, 64.93; H, 6.40; N, 9.88%. $C_{23}H_{27}N_3O_5$ requires C, 65.24; H, 6.60; N, 9.63%. FT-IR (ν_{max}/cm^{-1}): 3305 (OH), 1857 (C=O), 1739 (C=O), 1638 [(NH)C=O(N)]. ^{1}H NMR (400 MHz, DMSO-*d*$_6$): δ_H 1.38 (3H, s, CH$_3$), 3.32 (4H, t, CH$_2$), 3.55 (4H, t, CH$_2$), 3.85 (2H, s, CH$_2$), 5.06 (2H, s, OH), 7.02–7.62 (8H, m, PhH), 8.61 (1H, s, NH). FABMS: *m*/*z* 425 (M$^+$)].

2.3. ***PU-PACY*** *and* ***PU-PAZ*** *polymers [illustrated in Scheme 3(a) and (b)]*

(a) DBTDL (several drops) was added to a solution of [G-1.5]-C18-Diol (0.884 g, 0.500 mmol) in dry DMF (5.00 mL). This mixture was then added dropwise over 3 h to a solution of MDI (0.250 g, 1.00 mmol) in DMF (5 mL) at 60 °C. After the addition of a catalytic amount of DMPO, heating of the solution was continued for 8 h. At this point, TMA (0.096 g, 0.500 mmol) was added to the mixture and then the reaction was continued under a N_2 atmosphere for 7 h. **PU-PACY** polymers were obtained after evaporation of the solvent. FT-IR (ν_{max}/cm^{-1}): 1852 (C=O), 1780 (C=O).

(b) DBTDL (several drops) was added to a solution of [G-1.5]-C18-Diol (0.884 g, 0.500 mmol) in dry DMF (5.00 mL). This mixture was then added to a solution of MDI (0.250 g, 1.00 mmol) in DMF (5.00 mL). The solution was heated at 60 °C for 3 h and then [G-0.5]-Diol was added under a N_2 atmosphere over a period of 1 h. **PU-PAZ** polymers were obtained after evaporation of the solvent. FT-IR (ν_{max}/cm^{-1}): 1855 (C=O), 1740 (C=O).

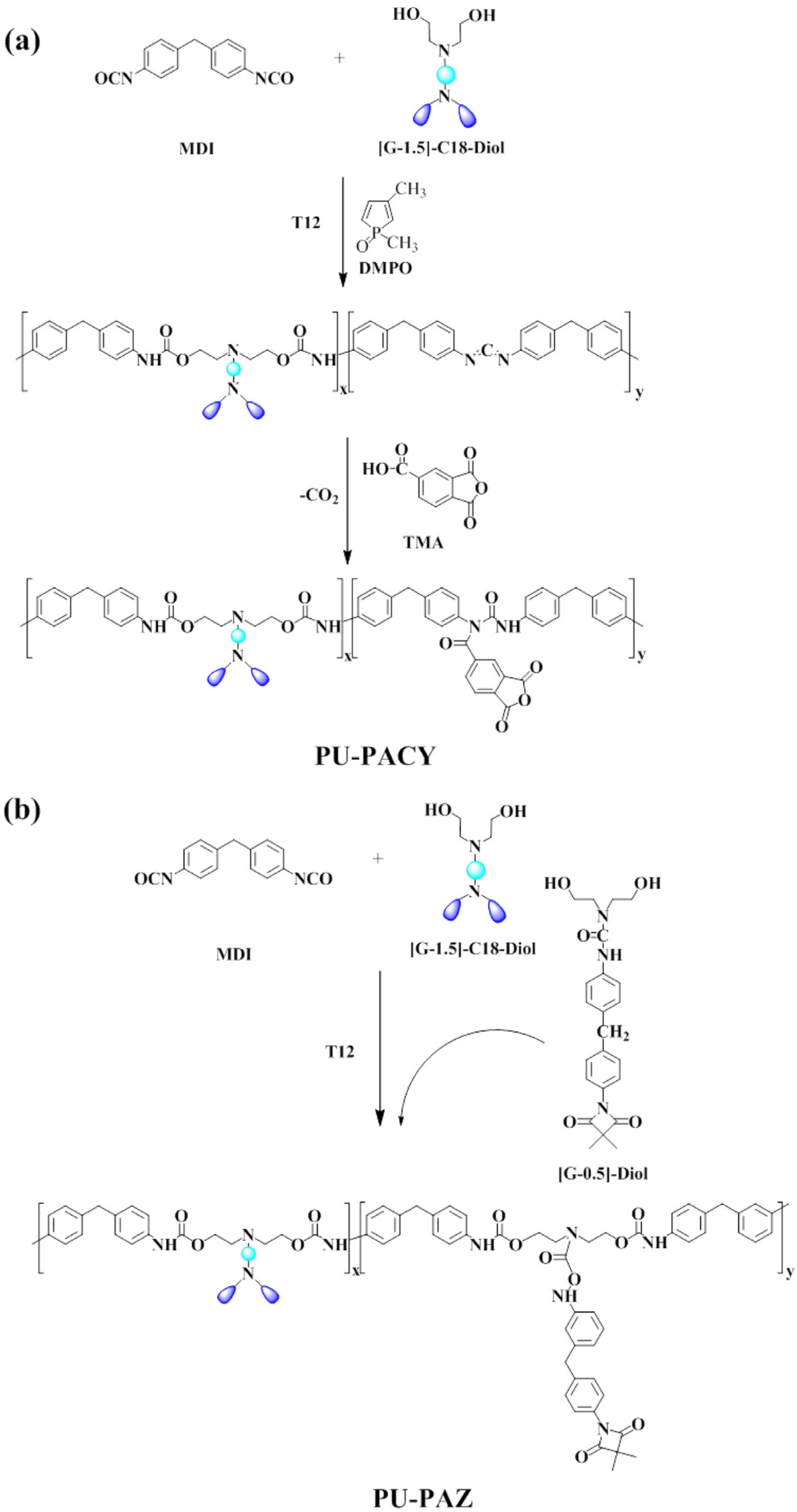

Scheme 3. Syntheses of (a) **PU-PACY** and (b) **PU-PAZ**.

2.4. All films prepared

(a) Thin films prepared through spin-coating: z solution of **PU-PACY** or **PU-PAZ** (20 mg/mL in $CHCl_3$) was spin-coated (2000 rpm) onto a silicon wafer.

(b) Honeycomb-like polymer films prepared through breath-figure processing: A solution of **PU-PACY** or **PU-PAZ** (10 mg/mL in chloroform) was cast onto a silicon wafer. The solvent was evaporated at room temperature under a flow of moist air (1 m/s). After complete evaporation of solvent, a white polymeric film, featuring a honeycomb-like morphology, was formed [illustrated in Scheme 4(a)].

(c) Hydrophobic or hydrophilic honeycomb-like PU films prepared through chemical modification: A **PU-PACY** or **PU-PAZ** honeycomb-like film was submerged for 24 h in a solution of M2005, M1000, or 1,6-diaminohexane in MeOH at 60 °C. After complete evaporation of the solvent, a white PU film, featuring a honeycomb-like morphology, was formed [illustrated in Scheme 4(b)].

(d) Rod-co-valley–like surfaces prepared through a peeling-off process: a rod-*co*-valley-like film was prepared by peeling off the first layer of a honeycomb-like film with a sheet of adhesive tape (Scotch Tape, 3M) [31] [illustrated in Scheme 4(c)].

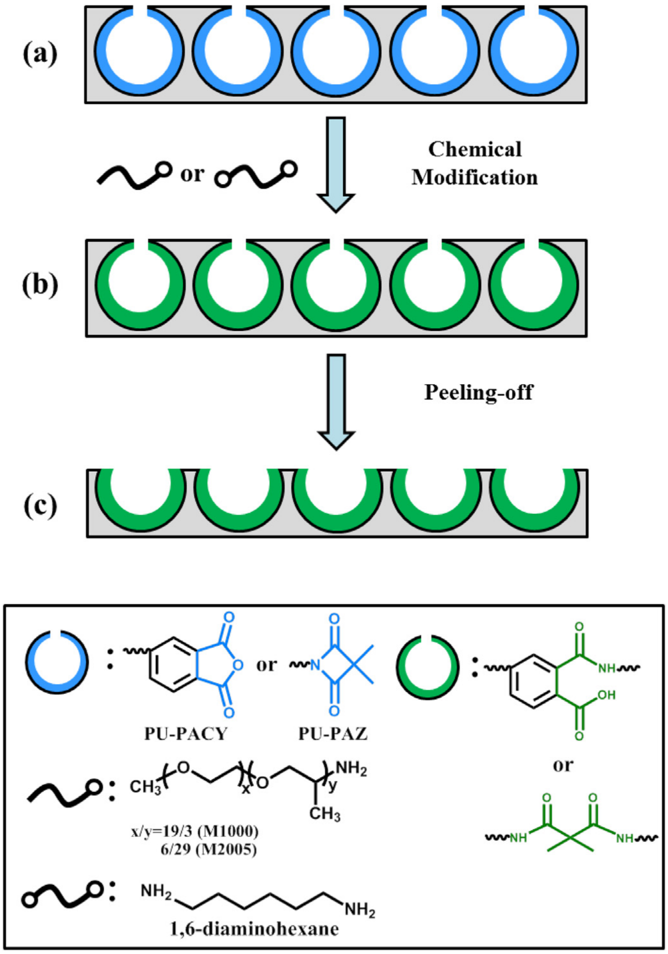

Scheme 4. Schematic representations of (a) the formation of the surface pores of the honeycomb-like films, (b) the chemical modification of the honeycomb-like films, and (c) the honeycomb-like films obtained after applying the peeling-off method.

2.5. Measurement

^1H NMR spectra of $CDCl_3$ and DMSO-d_6 solutions were recorded using a Varian Gemini-400 FT-NMR spectrometer. IR spectra were recorded using a PerkinElmer Spectrum One FT-IR spectrometer. Thermal analysis was conducted under N_2 using a TA Instrument DSC2010 apparatus operated at a heating rate of 10 °C/min. Thermogravimetric analysis (TGA) was performed using a Seiko SSC-5200 thermogravimetric analyzer operated at a heating rate of 10 °C/min under N_2. The thermal decomposition temperature (T_d) was taken to be the temperature corresponding to 5% weight loss of the sample. Fast atom bombardment mass spectrometry (FABMS) analysis was performed on a JEOL JMS SX/SX 102A mass spectrometer equipped with the standard FAB source, whose upper limit for measuring molecular weight is 2000. Gel permeation chromatography (GPC) was conducted using a Waters apparatus equipped with Waters Styragel columns and a refractive index detector (polystyrene calibration; mobile phase: THF). Scanning electron microscopy (SEM) of the films was performed using a field-emission scanning electron microscope (Hitachi S-5200) after the films had been sputtered with a thin layer of gold/palladium alloy. Average pore size (D) was measured from binary-contrasted SEM images by using an imaging software (ImageJ [64]). The tiny pores generated in the polymer frames were neglected. The contact angles (CAs) of water droplets (5 mL) on the films were measured at room temperature at 5-s intervals for 30 s using an optical contact angle meter (Kyowa DropMaster); all the measured CAs were constant during the 30-s period.

3. Results and discussion

3.1. Synthesis and characterization of the dendritic polymers **PU-PACY** and **PU-PAZ**

We used FT-IR spectroscopy to characterize the synthesized polymers **PU-PACY** and **PU-PAZ**. Our synthesis of **PU-PACY** involved the direct preparation of poly(urethane-*co*-carbodiimide) (PU-CDI) from the aromatic diisocyanate MDI and [G-1.5]-C18-Diol in the presence of DMPO catalyst and subsequent reaction of PU-CDI with the carboxylic acid of TMA at room temperature (Scheme 3a). After [G-1.5]-C18-Diol had been prepolymerized with MDI, the characteristic absorption peak of the residual isocyanate (NCO) units was evident at 2260 cm^{-1} in the FT-IR spectrum (Fig. 1). The addition of catalytic DMPO converted the NCO groups to CDI (N=C=N) units, with characteristic absorption peaks at 2106 and 2134 cm^{-1}. Subsequent reaction of the CDI units with the carboxylic (COOH) functionality of TMA gave the polyacylurea, with characteristic absorption peaks for the carbonyl (C=O) groups at 1715 cm^{-1} and the anhydride (C–O–C) groups at 1778 and 1857 cm^{-1}. The signals for the N-acylurea and anhydride linkages in the FT-IR spectra confirmed the successful preparation of **PU-PACY** based on the CDI chemistry [51–53] in Fig. 1(a). We prepared the **PU-PAZ** polymer by allowing the [G1.5]-C18-Diol-PU prepolymer to react with G0.5-Diol. First, we reacted MDI with [G-1.5]-C18-Diol to form the PU prepolymer (Scheme 3b); we subsequently reacted the chain extender [G-0.5]-Diol featuring azetidine-2,4-diones terminal groups with the PU prepolymer to form **PU-PAZ**. The disappearance of the signal ($\nu = 2260$ cm^{-1}) for the NCO groups and the appearance of signals for the azetidine-2,4-dione units ($\nu = 1740$ and 1855 cm^{-1}) in the FT-IR spectrum confirmed the successful preparation of **PU-PAZ** [Fig. 1(b)]. We used GPC to determine weight average molecular weights (M_w) for **PU-PACY** and **PU-PAZ**, which were in the range of 17,470–42,310 g/mol with polydispersities ranged from 3.74 to 3.92. Furthermore, thermal decomposition temperatures (T_d; 5% weight loss) of honeycomb-

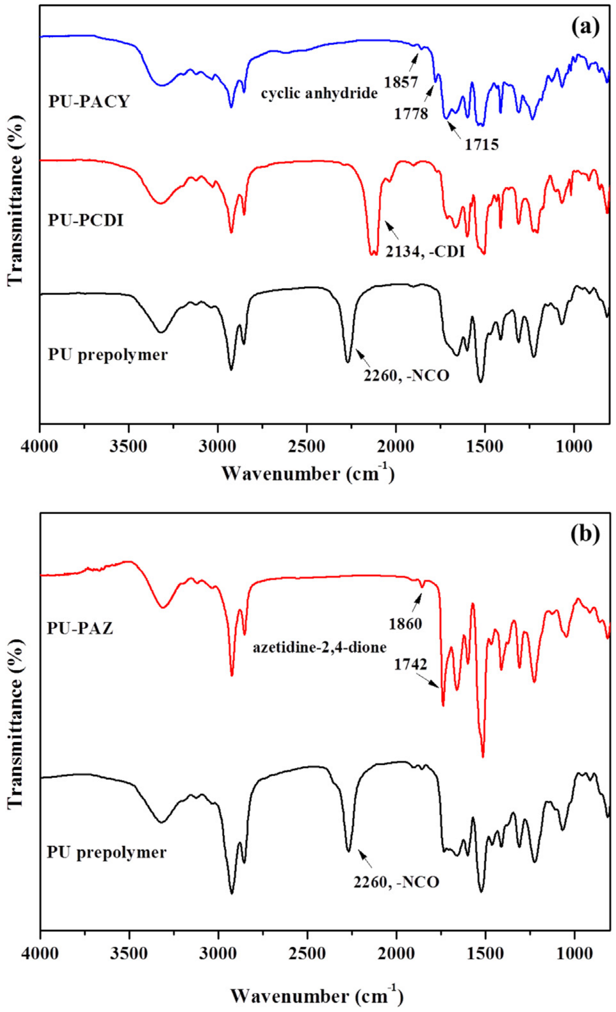

Fig. 1. FT-IR spectra of (a) **PU-PACY** and (b) **PU-PAZ**.

like films were in the range of 208–238 °C. The glass transition temperatures (T_g) of **PU-PAZ** samples ranged from 48.2 to 71.3 °C (Table 1).

3.2. Factors influencing the surface properties of **PU-PACY** films during film fabrication through the breath-figure process

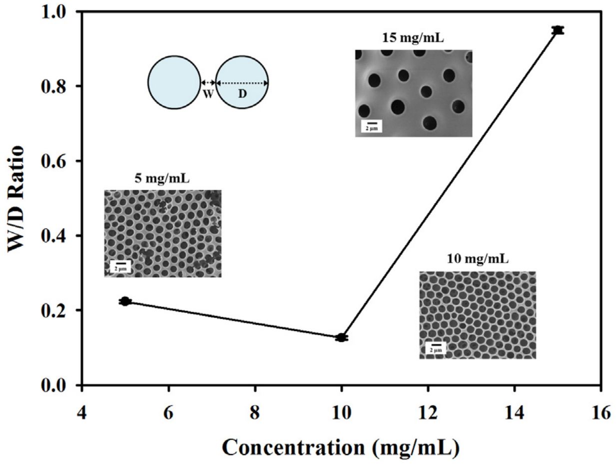

Fig. 2. SEM images demonstrating the pore distribution and uniformity on the surfaces of **PU-PACY** films prepared at polymer concentrations of 5, 10, and 15 mg/mL under 80% RH and their respective *W*/*D* ratios.

Deepak et al. reported the preparation of honeycomb-like polymeric films from a polymer presenting side chains having high molecular weight and hydrogen bonding functionality [16]. The self-formation of the honeycomb-like structure arose from the stabilization of water droplets through hydrogen bonding interactions at high humidity. For this current study, we designed two series of G1.5-C18 dendritic side-chain–grafted polymers with reactive functional groups, thereby enabling us to control the surface properties and manipulate the hydrophobicity of the honeycomb-like films.

Table 1
Physical properties of the **PU-PACY** and **PU-PAZ** honeycomb-like films.

Polymer	M_w (×0^3)	M_n (×10^3)	PDI	T_d[a] (°C)	T_g[b] (°C)
PU-PACY 50/50	17.47	4.61	3.79	208	n.d.[c]
PU-PACY 60/40	21.21	5.44	3.90	209	n.d.
PU-PACY 70/30	23.69	6.01	3.94	227	n.d.
PU-PAZ 50/50	29.33	7.84	3.74	233	71.3
PU-PAZ 60/40	33.46	8.65	3.87	235	60.6
PU-PAZ 70/30	4231	1080	392	238	482

[a] Temperature at which 5% weight loss occurred during TGA (N_2; heating rate: 10 °C/min).
[b] Determined through DSC analysis under N_2 (heating rate: 10 °C/min).
[c] Not detectable due to SSRR [51].

The surface properties of the films could be tailored by introducing pores at their surfaces. Previous reports have suggested that the ratio between the values of *W* and *D* can be correlated to the CA; specifically, a low *W*/*D* ratio generally indicates a high CA [25,26]. Accordingly, our first focus was to maximize the pore effect by varying the concentration of the polymer solution used to form the **PU-PACY** film. At 80% relative humidity (RH), we cast solutions of **PU-PACY** 70/30 (where "70/30" represents the molar ratio of PU to the dendritic polymer) of various polymer concentrations onto silicon wafers. SEM revealed that a polymer concentration of 5 mg/mL provided a film featuring broken, irregular pores ($W/D = 0.22$) distributed on its surface (Fig. 2), due to the low polymer concentration failing to self-stabilize in a highly humid environment. In comparison, at a higher concentration of 15 mg/mL, condensation of water was enhanced, resulting in the formation of large pores with a widened pore-to-pore distance and, thus, a high *W*/*D* ratio of 0.95 [38,39]. Thus, a low polymer concentration favored pore

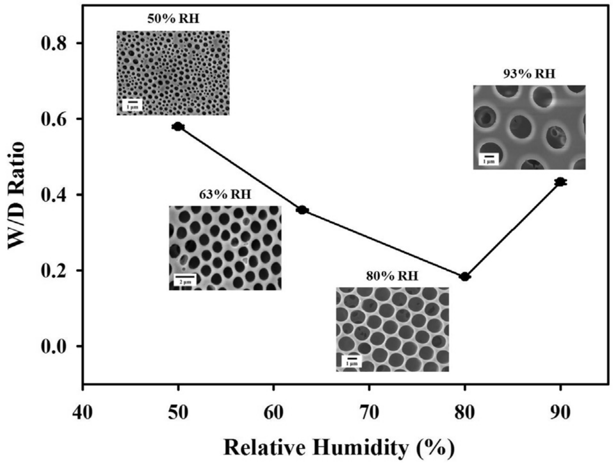

Fig. 3. SEM images demonstrating the pore uniformity on the surfaces of **PU-PACY** films prepared at a polymer concentration of 10 mg/mL under RHs of 50, 63, 80, and 93% and their respective *W*/*D* ratios.

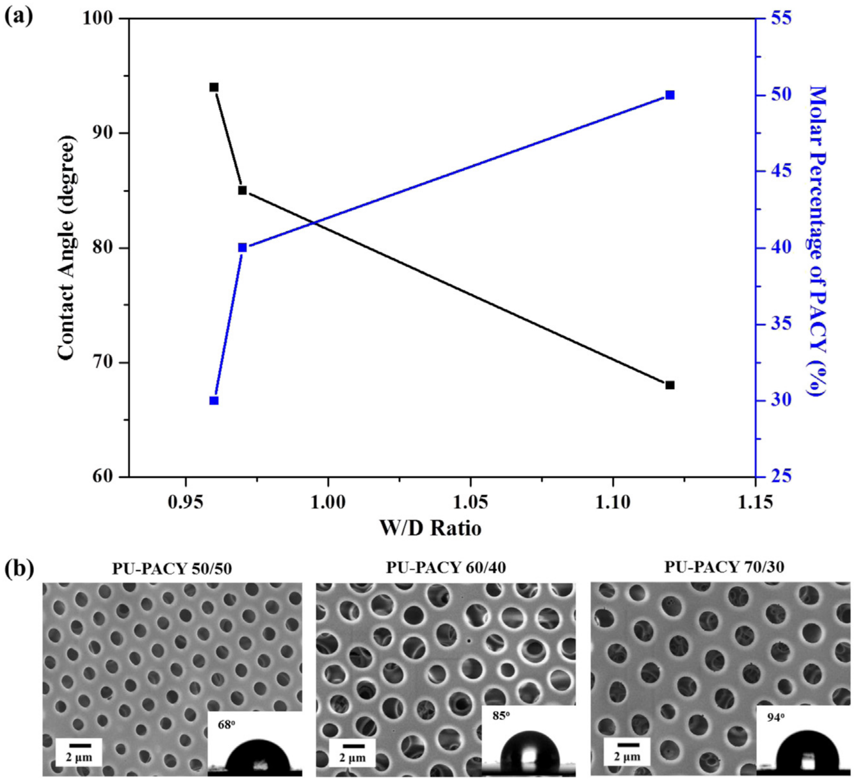

Fig. 4. (a) Inversely related CAs and molar percentages of the polymer **PACY** with respect to the *W*/*D* ratio. (b) SEM images revealing the pore uniformity on **PU-PACY** 50/50, 60/40, and 70/30 films and corresponding CAs.

formation, whereas a high concentration favored the formation of a honeycomb-like surface. Accordingly, when we tested an in-between value of 10 mg/mL for the polymer concentration, we successfully prepared – at 80% RH – a honeycomb-like film featuring uniformly sized and evenly distributed pores. As expected, this film had a *W*/*D* ratio of 0.13, lower than those of 0.22 and 0.95 for the films prepared at polymer concentrations of 5 and 15 mg/mL, respectively. Thus, the *W*/*D* ratio serves as an index to quantify the surface morphology of a honeycomb-like film, with a low value representing a film surface presenting a uniform distribution of evenly size pores.

With the **PU-PACY** 70/30 concentration optimized at 10 mg/mL, we next examined the influence of the RH during film preparation on the *W*/*D* ratio. As revealed in Fig. 3, the RH significantly affected the pore-to-pore distance, pore size, and uniformity. For example, at a low RH of 50%, the film surface featured scattered, nanoscale pores with a *W*/*D* ratio of 0.58. We attribute this behavior to the micro-sized water droplets having difficulty condensing on the film surface under such a comparatively low humidity. In contrast, under a relatively moisture-saturated RH of 90%, the *W*/*D* ratio decreased to 0.43, due to the inevitable collision and mutual condensation of water droplets resulting in larger pores and a wider distance between them [42]. By fine tuning the RH to 80%, we obtained a honeycomb-like film featuring uniform pores and a *W*/*D* ratio of 0.18.

Having optimized the film forming conditions at a polymer concentration of 10 mg/mL and an RH of 80%, we examined the effect of the polymer composition on the pores and on the CAs of the surfaces. Fig. 4(a) plots the CAs and percentages of **PACY** in the overall composition with respect to the *W*/*D* ratios. The *W*/*D* ratios and the CAs were inversely related over the entire range of polymer compositions. For example, at 30 mol% of **PACY**, the *W*/*D* ratio of the honeycomb-like film and the CA of the film surface were 0.96 and

Table 2
Molar compositions, *W*/*D* ratios, and CAs of the **PU-PACY** and **PU-PAZ** honeycomb-like films.

Polymer	Composition (molar ratio)				Rim width *W* (μm)[a]	Pore size *D* (μm)	*W*/*D*	CA (°)
	MDI	[G-1.5]-C18-Diol	[G-0.5]-Diol	TMA				
PU-PACY 50/50	1	0.5	–	0.5	1.19	1.06	1.12	68
PU-PACY 60/40	1	0.6	–	0.4	1.74	1.79	0.97	85
PU-PACY 70/30	1	0.7	–	0.3	1.72	1.79	0.96	94
PU-PAZ 50/50	1	0.5	0.5	–	0.855	1.32	0.65	101
PU-PAZ 60/40	1	0.6	0.4	–	0.769	1.48	0.52	105
PU-PAZ 70/30	1	0.7	0.3	–	0.565	1.74	0.32	113

[a] Rim width (*W*): measured along the hole center-hole center line.

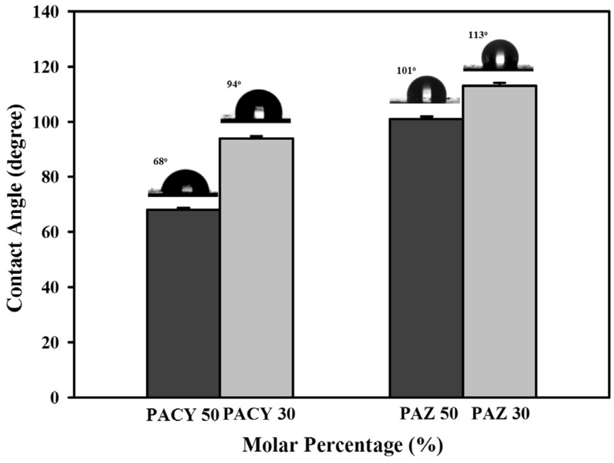

Fig. 5. A comparison of the CAs of the **PU-PACY** and **PU-PAZ** systems.

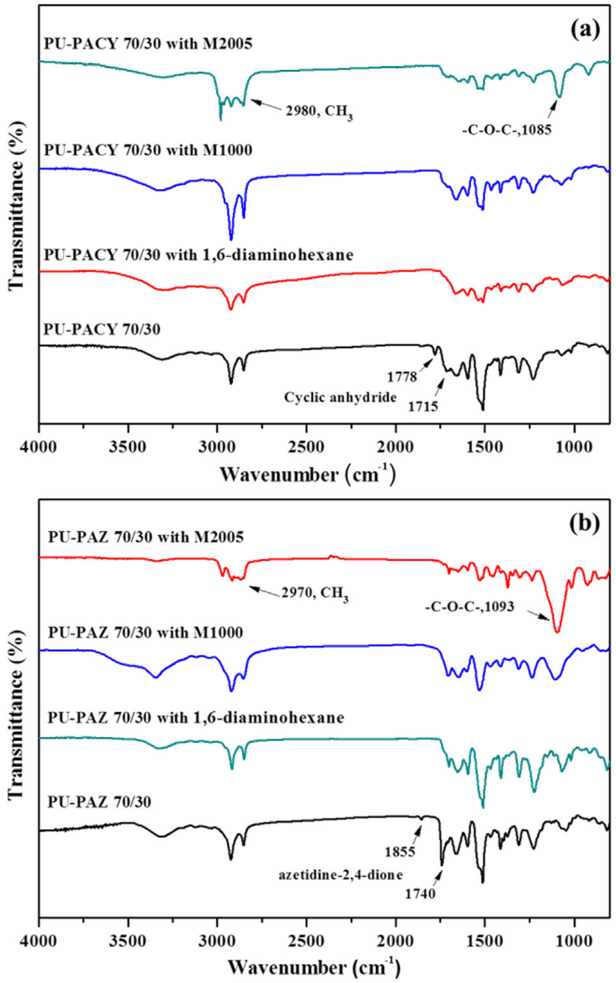

Fig. 6. FT-IR spectra of amine-modified (a) **PU-PACY,** and (b) **PU-PAZ** honeycomb-like films.

94°, respectively, while at 50 mol% the *W*/*D* ratio increased to 1.12, whereas the CA decreased to 68°.

These results for the **PU-PACY** system are significantly different from those we obtained in a previous study of a polystyrene (PS)-type system [45]. During the film forming process, PS could not effectively stabilize the water droplets, due to aggregation of the micro-sized water droplets into large particles. In comparison, the PU-type polymer has backbone functionalities that can partake in additional hydrogen bonding interactions at the water–polymer solution interface to help stabilize the water droplets; these additional interactions enhanced the formation of small pores with a wide pore-to-pore distance. Furthermore, the presence of the dendron units also offered additional hydrogen bonding sites. Because a decrease in the molar percentage of **PACY** implies an increase in the content of dendron molecules, a polymer composition featuring a low molar percentage of **PACY** resulted in a low *W*/*D* ratio and, inversely, a high CA. Our results are in good agreement with those reported by Yabu, who demonstrated a general trend of decreasing rim width (*W*) and increasing pore sizes (*D*) correlating with higher CAs [25].

3.3. *Effect of hydrophobic/hydrophilic functionalities of PU polymers on CAs*

During the breath-figure process, the presence of an amphiphilic copolymer can facilitate the formation of honeycomb-like films [18]. The balance between the number of hydrophobic and hydrophilic moieties significantly affects the surface tension between the polymer solution and water molecules. Thus, we prepared the polymer **PU-PAZ** as a control for comparison of its properties with those of **PU-PACY**. The structure of **PU-PAZ** features azetidine-2,4-dione functional groups, making it relatively more hydrophobic than **PU-PACY**. At the set conditions of a polymer concentration of 10 mg/mL and an RH of 80%, we evaluated the CAs of the respective polymer films (Table 2 and Fig. 5). In general, the CAs of the **PU-PAZ** polymers were higher than those of their **PU-PACY** analogues. For example, the film of **PU-PACY** 70/30 exhibited a CA of approximately 94°, whereas its **PAZ** analogue had a higher value of 113°. We suspect that the relatively more hydrophobic azetidine-2,4-dione functionalities in the structure of **PAZ** increased the degree of repulsion between the organic polymer solution and the water molecules, thereby increasing the CAs.

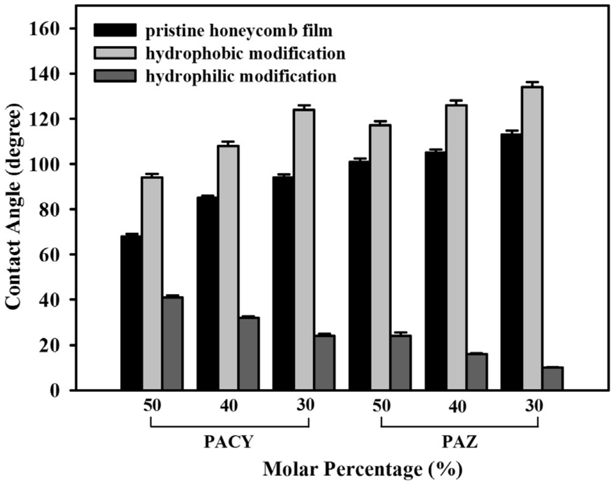

Fig. 7. CAs of **PU-PACY** and **PU-PAZ** honeycomb-like films modified through reactions with hydrophilic M1000 and hydrophobic M2005.

3.4. *Surface modification of the honeycomb-like films through a chemical approach*

Tsujii et al. reported that a fractal structure generated from hydrophobic wax crystals could strongly repel water [65]. Hosono et al. also demonstrated that the water CA on inorganic nanopins coated with hydrophobic surfactants could reach as high as 178° [66]. Generally, the wettability of a surface can change drastically depending on its chemical properties. Accordingly, we further tailored the surface properties of our honeycomb-like **PU-PACY** and **PU-PAZ** films through reactions with hydrophobic M2005, hydrophilic M1000, and 1,6-diaminohexane. The FT-IR spectra in Fig. 6(a) reveal that when the amines opened the rings of the cyclic anhydride units in the dendritic **PACY**, the characteristic absorption peaks of the anhydride groups originally at 1715, 1778, and

Table 3
Solvent-resistances of the crosslinked honeycomb-like films in various solvent systems at 60 °C for 24 h.

Polymer	THF	$CHCl_3$	Acetone	DMF
PU-PACY 50/50	−−	−−	−−	+−
PU-PACY 60/40	−−	−−	−−	+−
PU-PACY 70/30	+−	+−	+−	++
PU-PAZ 50/50	−−	−−	−−	−−
PU-PAZ 60/40	−−	−−	−−	+−
PU-PAZ 70/30	−−	+−	−−	++

++: Soluble; +−: partially soluble; −−: insoluble.

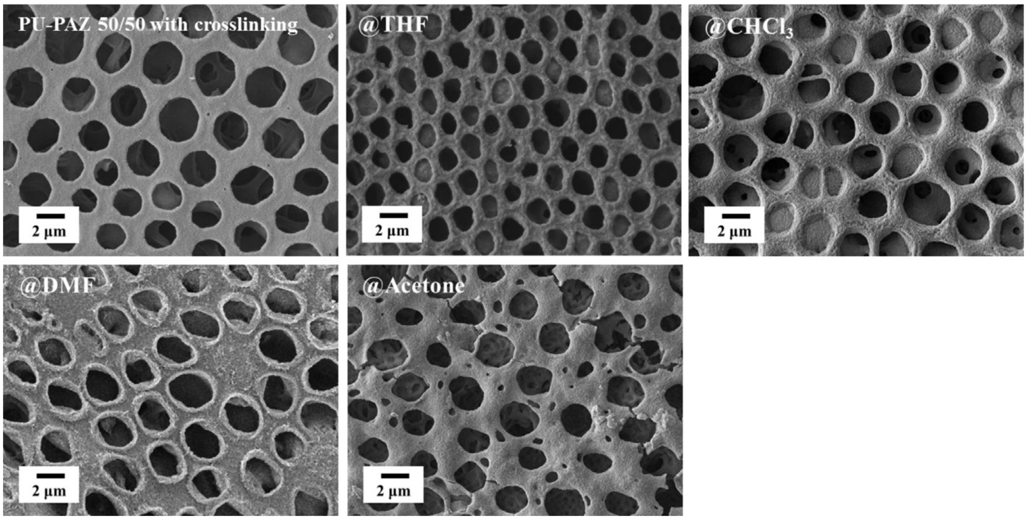

Fig. 8. SEM images of crosslinked **PU-PAZ** 50–50 before and after solvent treatment.

1850 cm^{-1} disappeared [67]. Similarly, we used the same amines to modify the **PU-PAZ** analogues. The characteristic absorption peak of the azetidine-2,4-dione units originally at 1740 and 1855 cm^{-1} also disappeared (Fig. 6(b)) [54]. For both **PU-PACY** and **PU-PAZ**, the disappearance of these characteristic absorption peaks was evidence for successful chemical modifications of their film surfaces.

We performed surface modifications through reactions with M1000 and M2005 because of their similar propylene oxide/ethylene oxide (PO/EO) backbones but different PO/EO ratios. Both the **PU-PACY** and **PU-PAZ** films modified with the PO-rich M2005 had, in general, higher CAs than their pristine honeycomb-like films (Fig. 7), presumably because the highly hydrophobic PO units decreased the affinity of the film toward water. In comparison, reactions with the EO-rich M1000 decreased in CAs because of strong interactions between the hydrophilic EO units and water droplets. Thus, we could readily manipulate the surface properties of these honeycomb-like films through chemical modification with hydrophobic/hydrophilic monoamines.

In contrast, modification with 1,6-diaminohexane did not change the CAs of the films because of the absence of PO and EO segments in the structure. Indeed, reactions with this difunctional amine afforded honeycomb-like films with urea-crosslinked structures favorable for solvent-resistance. We immersed the crosslinked films in the polar solvents THF, CHCl$_3$, acetone, and DMF at 60 °C for 24 h to test their solubilities; we found (Table 3) that the film of **PU-PAZ** 50/50 exhibited dramatic improvements in stability against these four solvents. SEM images of the urea-crosslinked structure (**PU-PAZ** 50/50) revealed that the honeycomb films were slightly swollen after THF and CHCl$_3$ solvent treatments (Fig. 8). However, the swollen effect was more pronounced when treated by DMF and Acetone.

3.5. Surface modification of the hydrophobic honeycomb-like films through a physical approach

The pristine thin **PU-PAZ** film exhibited a low CA of less than 100° (Fig. 9). By employing the breath-figure process for film formation, the resulting **PU-PAZ** honeycomb-like film featured a porous surface exhibiting a CA of 113°. When we further chemically modified the **PU-PAZ** honeycomb-like film through reaction with the hydrophobic M2005 to decrease its surface energy, the CA increased to 134° because of the presence of PO segments in the backbone of the poly(oxyalkylene)amine M2005. The water-repellency of the hydrophobic **PU-PAZ** honeycomb-like films could be enhanced further to superhydrophobicity through a physical approach involving the creation of a rough, nanoscopic architecture on the surface. This process involved peeling off the first thin layer of the films to introduce a rod-*co*-valley–like 3D surface. The lengths and diameters of the rods ranged from 1 to 2 µm and from 250 to 300 nm, respectively. In this study, the combination of a rod-*co*-valley–like 3D morphology and sub-micrometer arrays increased the CA to 151°. Obviously, the apparent CAs increase with surface roughness compared with a CA value of 94° on the flat thin film of **PU-PAZ.** The relationship between contact angle and rough topography was analyzed via the Cassie–Baxter equation: $\cos\theta_1 = f_1 \cos\theta_2 - f_2$ [68,69], where θ_1 and θ_2 are the CAs on the flat thin film surface (spin-coating film) and (including honeycomb-like film, hydrophobicity honeycomb-like film or rod-co-valley-like film), respectively, f_1 and f_2 are the fractions of liquid in respective contact with solid and air at the interfaces ($f_1 + f_2 = 1$). After calculation, the $f_{1,\ \text{honeycomb}}$ and the $f_{1,\ \text{hydrophobicity honeycomb}}$ were 0.655 and 0.328, respectively. In particular, the $f_{1,\ \text{rod-co-valley}}$ was dramatically decreasing to 0.135, indicating that a much smaller portion of solid contacting with water was found on the rod-co-valley surface.

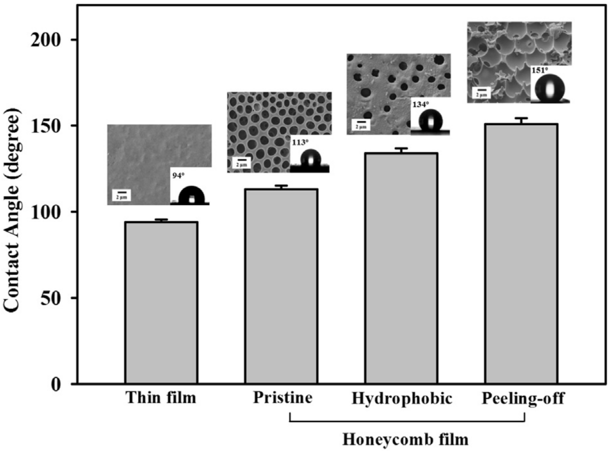

Fig. 9. CAs and surface morphologies of chemically and physically modified **PU-PAZ** honeycomb-like films.

4. Conclusion

We have synthesized two functional PU polymers grafted with a series of waxy dendrons, which feature a focal part rich in hydrogen bonding groups and peripheral nonpolar units offering van der Waals interactions. The **PU-PACY** and **PU-PAZ** polymers were functionalized with pendent anhydride and azetidine-2,4-dione units, respectively. Processing of the resulting polymers led to their self-assembly into honeycomb-like films with controllable *W*/*D* ratios. The presence of the azetidine-2,4-dione pendent units caused the **PU-PAZ** species to be more hydrophobic than their anhydride-presenting **PU-PACY** analogues. Thus, the **PU-PAZ** honeycomb-like film exhibited a relatively high CA of 113° and a low *W*/*D* ratio of 0.32. When we further modified the **PU-PAZ** film with the hydrophobic poly(oxyalkylene)amine M2005, the CA increased to 134°. A subsequent peeling-off process introduced a submicrometer rod-*co*-valley-like 3D morphology onto the film surface, further increasing the CA to 151°. We attribute the superhydrophobicity of this film to the combination of its hydrophobic composition and the set of chemical and physical modifications. Furthermore, we enhanced the solvent-resistance of the films by crosslinking them through treatment with a diamine. Using this approach, we could prepare superhydrophobic/superhydrophilic honeycomb-like films with relative ease. We are currently exploring the possible applications of these films in areas such as microanalysis, cell growth, and stent tissue engineering.

Acknowledgments

We thank the Chung-Shan Institute of Technology and the National Science Council (NSC) of Taiwan for financial support.

References

[1] Liu H, Szunerits S, Pisarek M, Xu W, Boukherroub R. ACS Appl Mater Interfaces 2009;1:2086–91.
[2] Guo Z, Liu W. Plant Sci 2007;172:1103–12.
[3] Gao L, McCarthy TJ. Langmuir 2006;22:2966–7.
[4] Feng L, Zhang Y, Xi J, Zhu Y, Wang N, Xia F, et al. Langmuir 2008;24:4114–9.
[5] Namavar F, Cheung CL, Sabirianov RF, Mei WN, Zeng XC, Wang G, et al. Nano Lett 2008;8:988–96.
[6] He JH, Liu Y, Xu L, Yu JY, Sun GC. Solitons Fractals 2008;37:643–51.
[7] Geim AK, Dubonos SV, Grigorieva IV, Novoselov KS, Zhukov AA, Shapoval SY. Nat Mater 2003;2:461–3.
[8] Yurdumakan B, Raravikar NR, Ajayanb PM, Dhinojwala A. Chem Commun; 2005. pp. 3799–801.
[9] Shi W, Zhang Y, Liu C, Wang Z, Zhang X. Langmuir 2008;24:1318–23.
[10] Brown PS, Talbot EL, Wood TJ, Bain CD, Badyal JPS. Langmuir 2012;28:13712–9.
[11] Peng CW, Chang KC, Weng CJ, Lai MC, Hsu CH, Hsu SC, et al. Polym Chem 2013;4:926–32.
[12] Ishii D, Shimomura M. Chem Mater 2013;25:509–13.
[13] Yabu H, Hirai Y, Kojima M, Shimomura M. Chem Mater 2009;21:1787–9.
[14] Widawski G, Rawiso M, Francois B. Nature 1994;369:387–9.
[15] Pitois O, Fracois B. Colloid Polym Sci 1999;277:574–8.
[16] Deepak VD, Asha SK. J Phys Chem 2006;110:21450–9.
[17] Fracois B, Pitois O, Franqois J. Adv Mater 1995;7:1041–4.
[18] De León AS, del Campo A, Fernández-García M, Rodríguez-Hernández J, Muñoz-Bonilla A. Langmuir 2012;28:9778–87.
[19] Wan LS, Lv J, Ke BB, Xu ZK. ACS Appl Mater Interfaces 2010;2:3759–65.
[20] Zhu Y, Sheng R, Luo T, Li H, Sun J, Chen S, et al. ACS Appl Mater Interfaces 2011;3:2487–95.
[21] Chen PC, Wan LS, Ke BB, Xu ZK. Langmuir 2011;27:12597–605.
[22] Ke BB, Wan LS, Xu ZK. Langmuir 2010;26:8946–52.
[23] Nurmawati MH, Renu R, Ajikumar PK, Sindhu S, Cheong FC, Sow CH, et al. Adv Funct Mater 2006;16:2340–5.
[24] Zhao B, Zhang J, Wang X. J Mater Chem 2006;16:509–13.
[25] Yabu H, Takebayashi M, Tanaka M, Shimomura M. Langmuir 2005;21:3235–7.
[26] Wu X, Wang S. ACS Appl Mater Interfaces 2012;4:4966–75.
[27] Kon K, Brauer CN, Hidaka K, Löhmannsröben HG, Karthaus O. Langmuir 2010;26:12173–6.
[28] Wong KH, Hernandez-Guerrero M, Granville AM, Davis TP, Barner-Kowollik C, Stenzel MH. J Porous Mater 2006;13:213–23.
[29] Connal LA, Vestberg R, Gurr PA, Hawker CJ, Qiao GG. Langmuir 2008;24:556–62.
[30] Stenzel-Rosenbaum MH, Davis TP, Fane AG, Chen V. Angew Chem Int Ed 2001;40:3428–32.
[31] Barner-Kowollik C, Dalton H, Davis TP, Stenzel MH. Angew Chem Int Ed 2003;42:3664–8.
[32] Zhang Z, Hughes TC, Gurr PA, Blencowe A, Uddin H, Hao X, et al. Polymer 2013;54:4446–54.
[33] Yabu H, Hirai Y, Shimomura M. Langmuir 2006;22:9760–4.
[34] Hernández-Guerrero Maribel, Min E, Barner-Kowollik C, Müllera AHE, Stenzel MH. J Mater Chem 2008;18:4718–30.
[35] Kim DG, Basavaraja C, Yamaguchi T, Huh DS. Polymer 2012;53:1347–54.
[36] Billon L, Manguian M, Pellerin V, Joubert M, Eterradossi O, Garay H. Macromolecules 2009;42:345–56.
[37] Yunus S, Delcorte A, Poleunis C, Bertrand P, Bolognesi A, Botta C. Adv Funct Mater 2007;17:1079–84.
[38] Ghannam L, Manguian M, Francois J, Billon L. Soft Matter 2007;3:1492–9.
[39] Kabuto T, Hashimoto Y, Karthaus O. Adv Funct Mater 2007;17:3569–73.
[40] Yabu H, Tanaka M, Ijiro K, Shimomura M. Langmuir 2003;19:6297–300.
[41] Liu C, Gao C, Yan D. Angew Chem Int Ed 2007;46:4128–30.
[42] Cheng C, Tian Y, Shi Y, Tang R, Xi F. Macromol Rapid Commun 2005;26:1266–72.
[43] Cheng CX, Tian Y, Shi YQ, Tang RP, Xi F. Langmuir 2005;21:6576–81.
[44] Hsieh SJ, Wang CC, Chen CY. Macromolecules 2009;42:4787–94.
[45] Ting WH, Chen CC, Dai SA, Suen SY, Yang IK, Liu YL, et al. J Mater Chem 2009;19:4819–41.
[46] Chang CC, Juang TY, Ting WH, Lin MS, Yeh CM, Dai SA, et al. Mater Chem Phys 2011;128:157–65.
[47] Karthaus O, Hashimoto Y, Kon K, Tsuriga Y. Macromol Rapid Commun 2007;28:962–5.
[48] Wang L, Maruf SH, Maniglio D, Ding Y. Polymer 2012;53:3749–55.
[49] Li L, Chen C, Li J, Zhang A, Liu X, Xu B, et al. J Mater Chem 2009;19:2789–96.
[50] Li L, Zhong Y, Li J, Chen C, Zhang A, Xu J, et al. J Mater Chem 2009;19:7222–7.
[51] Wei KL, Wu CH, Huang WH, Lin JJ, Dai SA. Macromolecules 2006;39:12–4.
[52] Chen AL, Wei KL, Jeng RJ, Lin JJ, Dai SA. Macromolecules 2011;44:46–59.
[53] Lin HL, Juang TY, Chan LH, Lee RH, Dai SA, Liu YL, et al. Polym Chem 2011;2:685–93.
[54] Dai SA, Juang TY, Chen CP, Chang HY, Kuo WJ, Su WC, et al. J Appl Polym Sci 2007;103:3591–9.
[55] Chang HY, Chao TY, Yang CC, Dai SA, Jeng RJ. Eur Polym J 2007;43:3988–96.
[56] Kuo MC, Tung YC, Yeh CL, Chang HY, Jeng RJ, Dai SA. Macromolecules 2008;41:9637–42.
[57] Liu YL, Wu YH, Jeng RJ, Dai SA. J Colloid Interface Sci 2009;336:189–94.
[58] Shau SM, Chang CC, Lo CH, Chen YC, Juang TY, Dai SA, et al. ACS Appl Mater Interfaces 2012;4:1897–908.
[59] Chen CP, Dai SA, Chang HL, Su WC, Jeng RJ. J Polym Sci Part A: Polym Chem 2005;43:682–8.
[60] Tsai CC, Juang TY, Dai SA, Wu TM, Su WC, Liu YL, et al. J Mater Chem 2006;16:2056–63.
[61] Liu JK, Shau SM, Juang TY, Chang CC, Dai SA, Su WC, et al. J Appl Polym Sci 2011;120:2411–20.
[62] Juang TY, Tsai CC, Wu TM, Dai SA, Chen CP, Lin JJ, et al. Nanotechnology 2007;18:205606–13.
[63] Tsai CC, Chang CC, Yu CS, Dai SA, Wu TM, Su WC, et al. J Mater Chem 2009;19:8484–94.
[64] Rasband WS. ImageJ. Bethesda, Maryland, USA: U. S. National Institutes of Health; 1997–2013. http://rsb.info.nih.gov/ij/.
[65] (a) Shibuichi S, Onda T, Satoh N, Tsujii K. Langmuir 1996;12:2125–7;
(b) Yan H, Kurogi K, Mayama H, Tsujii K. Angew Chem Int Ed 2005;44:3453–6.
[66] Hosono E, Fujihara S, Honma I, Zhou H. J Am Chem Soc 2005;127:13458–9.
[67] Lin JJ, Hsu YC, Wei KL. Macromolecules 2007;40:1579–84.
[68] Zhao N, Xie Q, Kuang X, Wang S, Li Y, Lu X, et al. Adv Funct Mater 2007;17:2739–45.
[69] Cassie A, Baxter S. Trans Faraday Soc 1944;40:546–51.